ADSORPTION OF URANIUM FROM AQUEOUS SOLUTION BY $Cu_{0.5}Ni_{0.5}Fe_2O_4$ – REDUCED GRAPHENE OXIDE NANOCOMPOSITES

Tran Quang Dat*, Nguyen Van Toan, Pham Van Thin, Do Quoc Hung

Le Quy Don Technical University, 236 Hoang Quoc Viet Street, Hanoi, Viet Nam.

*Email: *dattqmta@gmail.com*

Received: 15 July 2016; Accepted for publication: 2 December 2016

ABSTRACT

$Cu_{0.5}Ni_{0.5}Fe_2O_4$ – reduced graphene oxide composites (CNF-rGO) as an efficient adsorbent for the adsorption of uranium (VI) have been synthesized by a two-steps methods. The structures and the physicochemical properties of adsorbents are characterized by Scanning electron microscopy (SEM), X-ray diffraction (XRD), Raman spectroscopy (RAMAN) and Vibrating sample magnetometer (VSM) measurement. It was found that rGO were exfoliated and decorated homogeneously with CNF nanoparticles having diameters of 20 nm. The saturated magnetization (Ms) value was estimated to be 60 emu/g, remanences (Mr) and coercive forces (Hc) near to zero, indicating that obtained material is superparamagnetic. The *pH* effect, contact time and adsorption isotherms were examined in batch experiments. The adsorption isotherm agreed well with the Langmuir model, having a maximum adsorption capacity of 256 mg/g, at $pH = 6$, $T = 298$ K.

Keywords: reduced graphene oxide, $Cu_{0.5}Ni_{0.5}Fe_2O_4$, nanocomposites, uranium, adsorption.

1. INTRODUCTION

Hexavalent actinides constitute a significant proportion of the radioactive species distributed in nuclear waste, and are generated in the post-processing of spent fuels every year. Uranium is a toxic heavy metal arising from the nuclear industry as well as from anthropogenic activities. The hexavalent uranyl ion (UO_2^{2+}) is found to be the most stable form in vivo, and its compounds can cause irreversible renal injury and potential carcinogens [1]. Removal of U(VI) from aqueous solutions is very important. There are various methods to treat U(VI) from aqueous solutions, such as chemical precipitation, membrane dialysis, solvent extraction, flotation and adsorption [2]. Among all those processes, adsorption is probably the most common method in practical use. Highly-efficient adsorbents would enable the collection of trace-level metal ions from aqueous systems, thus improving the present technological levels of radioactive pollutant removal. Development of novel adsorbents with high adsorption capacity, fast adsorption kinetics, and easy separation and regeneration is in great demand.

Recently, the application of carbon-based nanomaterials in water treatment plants has

attracted significant attention due to the advantages of large surface areas and more activated functionalized sites [3, 4]. Graphene is receiving intense attention, driven by its unique physical and chemical properties. Graphene and graphene oxide have been reported as efficient adsorbents [5].

Over the years, magnetic adsorbents have emerged as a new generation of materials for environmental decontamination, since magnetic separation simply involves applying an external magnetic field to extract the adsorbents [6, 7, 8, 9]. Compared with traditional methods, such as filtration, centrifugation or gravitational separation, magnetic separation requires less energy and can achieve better separation especially for adsorbents with small particle sizes. Recently, ferrites have been employed in water purification [10].

Few years recently, some researchers have managed to fabricate magnetic graphene nanocomposites [11, 12]. The ferrite – rGO nanocomposite possesses attractive properties that could see potential use in catalysis, biomedicine, lithiumion batteries and sorbent for uranium or other actinides.

In this study, copper - nickel ferrite ($Cu_{0.5}Ni_{0.5}Fe_2O_4$) - reduced graphene oxide nanocomposites were synthesized for removal of U(VI) from aqueous solution. The adsorption properties of the adsorbent toward U(VI) in aqueous solution were investigated for adsorption capacity, contact time and effect of *pH*.

2. EXPERIMENTAL

2.1. Synthesis of reduced Graphene Oxide (rGO)

Graphite oxide was synthesized from graphite powder by a modified Hummers method [13]. The detailed processing is described as below: 1 g of graphite (99%) and 0.5 g of $NaNO_3$ were mixed with 50 mL of H_2SO_4 (98%) in a threenecked flask at 0°C. The mixture was stirred for 1 h. Then 3g of $KMnO_4$ was added to the suspension and the mixture was stirred at 10 °C for 2 h. The suspension was stirred at room temperature for 25 min followed by 5 min sonication in an ultrasonic bath. After repeating the stirring-sonication process for 12 times, the reaction was quenched by the addition of 200 mL distilled water. An extra 2 h ultrasonic treatment was carried out. After adjusting the *pH* at ~ 6 by the addition of 1 mol/L sodium hydroxide solution, the suspension was further sonicated for 1 h. 20 g L-ascorbic acid was dissolved in 200 mL distilled water and then was slowly added to the exfoliated graphite oxide suspension at room temperature. The reduction was performed at 95 °C for 1 h. The resultant black precipitates were simply filtered by filter paper and further were washed with a 1 mol/L hydrochloric acid solution and distilled water to neutral *pH*. Finally, the filtrate was freeze-dried to obtain rGO powder.

2.2. Synthesis of $Cu_{0.5}Ni_{0.5}Fe_2O_4$ - reduced Graphene Oxide composites (CNF - rGO)

Firstly, 4 mmol of $FeCl_3.\ 6H_2O$, 1 mmol of $NiCl_2.\ 6H_2O$ and 1 mmol of $Cu(NO_3)_2.\ 3H_2O$ were dissolved in a mixture of 60 mL of ethylene glycol and 40 mL of distilled water. Then, an appropriate amount of aqueous rGO (100 mg rGO/10 mL distilled water) and 4 mL of ammonia solution (25 %) were added to the mixture with stirring for 4 h. The resulting solution was then poured into a 150 mL Teflon-lined autoclave and heated to 190 ^{0}C, and kept at that temperature for 24 h. After cooling to room temperature, the precipitate was collected by magnet and washed repeatedly with distilled water and ethanol; it was then dried for 12 h at 60 ^{0}C.

2.3. Characterization and adsorption experiments

The morphologies and crystal structures of the CNF - rGO composites were characterised using Scanning electron microscopy (SEM - S4800, at Institute of Materials Science, Vietnam Academy of Science and Technology), X-ray diffraction (XRD, Bruker D5 with Cu $K_{\alpha 1}$ radiation λ = 1.54056 Å, at Hanoi University of Science) and Raman spectroscopy (LabRAM HR 800, excited by a 610 nm laser, at Hanoi University of Science). Magnetic measurements were performed with a vibrating sample magnetometer (VSM, DMS 880 in magnetic fields up to 13.5 kOe, at Hanoi University of Science).

A batch technique was applied to study the adsorption of U(VI) from aqueous solutions by CNF - rGO. A stock solution of uranium was prepared by dissolving $UO_2(NO_3)_2.6H_2O$ in deionized water. All batch experiments were conducted using CNF - rGO powders in a 100 mL conical flask with 50 mL of U(VI) aqueous solutions on a rotary shaker at 200 rpm at 298 K. At the end of the adsorption period, the suspension was isolated by using an external magnetic field. Then, the samples were filtered and the U(VI) concentration in the effluent was determined by an Inductively coupled plasma mass spectrometry (ICP-MS, Agilent 7500, at Institute for Technology of Radioactive and Rare Elements). The effect of *pH* on adsorption was studied in adsorption experiments using 20 mg of adsorbent in 50 mL of U(VI) solution (50 mg/L) and equilibrium time of 240 min. Different *pH* values ranging from 4 to 10 were adjusted by adding 0.1 mol/L NaOH or 0.1 mol/L HNO_3 solutions. We studied the effect of contact time on adsorption capacity, under the conditions: 20 mg of adsorbent, 50 mL of U(VI) solution (50 mg/L), *pH* = 6 and temperature 298 K. Different contact time was varied from 15 min to 360 min. In adsorption equilibrium isotherm studies, the initial concentrations of U(VI) were varied and the other parameters were kept constant (20 mg of adsorbent, contact time = 240 min and *pH* = 6).

The adsorption capacity of U(VI) was calculated according to the following equation:

$$Q_{eq} = \frac{C_0 - C_{eq}}{m} V \quad (1)$$

where Q_{eq} (mg/g) is adsorption capacity, C_0 and C_{eq} (mg/L) are the initial and equilibrium concentrations of uranium(VI) solution, m is the weight of sorbent (g), V is the volume of the uranium(VI) solution (L).

3. RESULTS AND DISCUSSION

3.1. Characterization of samples

Fig. 1 shows the SEM image of rGO. Well-exfoliated but crumpled and aggregated rGO sheets are observable in the SEM image. Fig. 2 shows the SEM images of the CNF – rGO nanocomposites. It can be seen that the $Cu_{0.5}Ni_{0.5}Fe_2O_4$ nanoparticles are uniformly dispersed on the surface of the graphene sheets and between the layers of the graphene sheets. It exhibited uniform, almost spherical shaped and loosely agglomerated particles of $Cu_{0.5}Ni_{0.5}Fe_2O_4$ ferrite, and the particle size is quite homogenous about of 20 nm.

In the XRD pattern of rGO (Fig. 3), we can see a broad peak corresponding to rGO at about 24.44^0, with an interlayer spacing of 3.6 nm. Fig. 4 shows the XRD patterns of the CNF – rGO

composites. The broad and well defined diffraction peaks were observed at 2θ = 18.49, 30.37, 35.62, 37.27, 43.3, 53.65, 57.31, 62.86 degrees, corresponding to (111), (220), (311), (222), (400), (422), (511) and (440) planes, respectively. X-ray diffraction data identified that the $Cu_{0.5}Ni_{0.5}Fe_2O_4$ particles have face-centered cubic trevorite structure. The estimated value of lattice constants was found to be a = 8.34 Å. The estimated value of particle size of the particles is found to be about 20 nm.

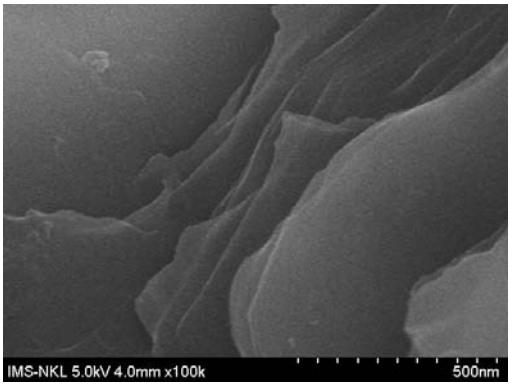

Figure 1. SEM image of rGO.

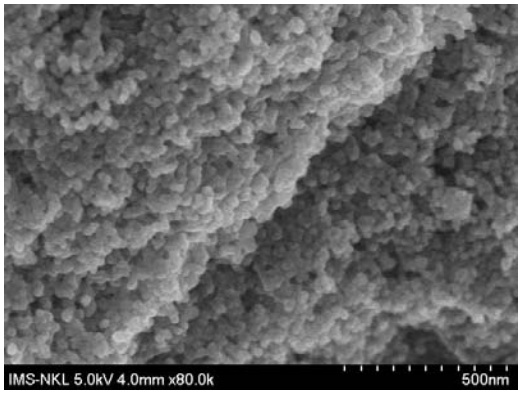

Figure 2. SEM image of CNF - rGO composites.

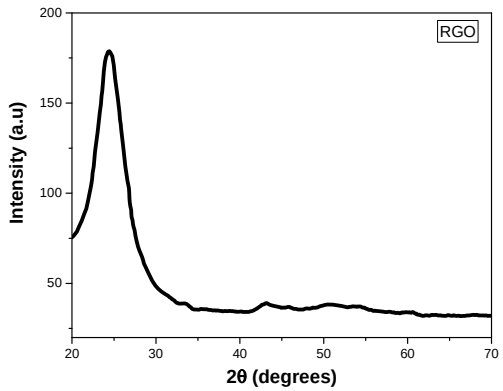

Figure 3. XRD patterns of rGO.

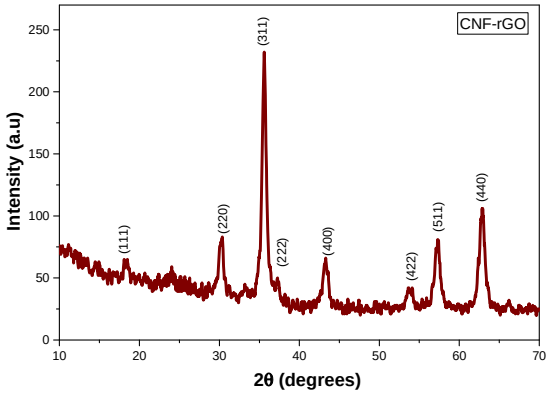

Figure 4. XRD patterns of CNF – rGO composites.

Raman spectroscopy is also one of the most sensitive and informative techniques to characterize disorder in sp^2 carbon materials. As shown in Fig. 5a, for rGO, the Raman peaks of the G-band (1582 cm^{-1}) and D-band (1325 cm^{-1}) have found. The G band arose from the first-order scattering of the E_{2g} mode of carbon sp^2 atoms, while the D band was due to the K-point phonons of the A_{1g} mode and was associated with the vibration of sp^3 carbon domains typical of disordered graphite [14]. Comparing with the Raman spectrum of the rGO, it is obvious to see that the Raman peaks of G- and D-bands in the Raman spectra of the CNF-rGO nanocomposites shift to lower frequencies. The D-band shifted from 1325 cm^{-1} to 1315 cm^{-1} while the G-band shifted from 1582 cm^{-1} to 1569 cm^{-1}, indicating that GO had been reduced to graphene.

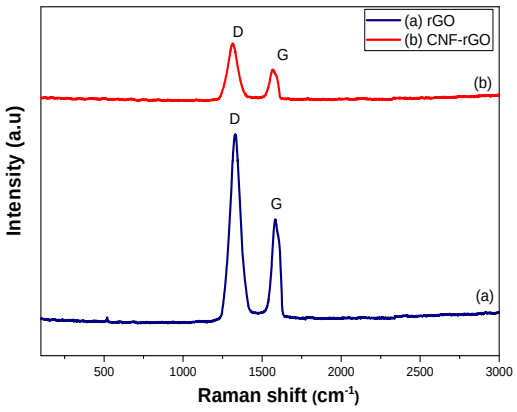

Figure 5. Raman spectra of (a) rGO and (b) CNF-rGO excited by a 610 nm laser.

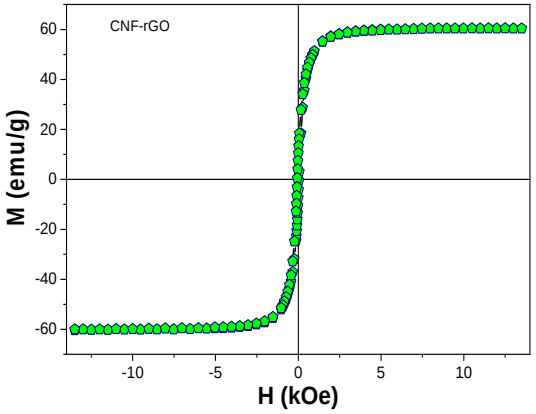

Figure 6. Room temperature magnetic hysteresis loops of the CNF – rGO composites.

Room temperature magnetization for CNF - rGO composites was investigated and is shown in Fig. 6. The magnetization of samples increases with external magnetic field strength. The VSM measurement had shown that obtained material was typically superparamagnetic with remanences (*Mr*) and coercive forces (*Hc*) being near to zero. The saturated magnetization (Ms) value was estimated to be 60 emu/g. A large saturation magnetization makes this adsorbent easy to separate from solution by applying an external magnetic field.

3.2. Effect of initial *pH*

The effect of solution *pH* on the adsorption capacity of CNF - rGO composites for U(VI) was illustrated in Fig. 7. The removal of uranium sharply increases from 100.5 mg/g to 117.5 mg/g when the *pH* increases from 4 to 6. If the *pH* value was continually enhanced from 6 to 10, the adsorption ability starts decreasing. This result indicates that the adsorption ability of CNF - rGO for U(VI) is strong in near neutral circumstance. The maximum adsorption yield was observed at $pH = 6$.

At low *pH* of solution, the uranium (VI) is present mainly in the form of free $[UO_2]^{2+}$ ions and the binding sites of CNF - rGO may become positively charged due to the protonation reaction. The adsorption process is not favored. Moreover, excess H^+ occupies many adsorption sites. At $pH > 6$, the surface charge of sorbents became more negative and uranium is present as anionic species such as $[UO_2(OH)_3]^-$, $[UO_2(OH)_4]^{2-}$… The repulsion between uranium anions and sorbents with surface negative charges resulted in the drop of U(VI) adsorption. Similar results were also reported for U(VI) adsorption [11]. Consequently, $pH = 6$ is considered as the optimum *pH* for further experiments.

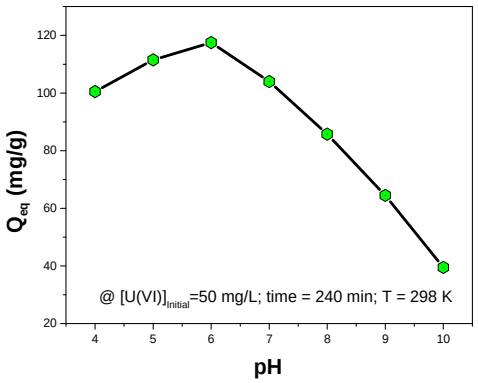

Figure 7. Effect of *pH* on adsorption of uranium.

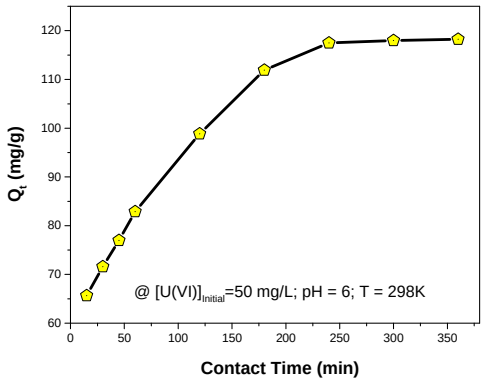

Figure 8. Effect of contact time on adsorption of uranium.

3.3. Effect of contact time on uranium adsorption

Figure 8 presents the amount of uranium adsorption on CNF - rGO nanocomposites as a function of contact time. The equilibrium is established after 240 min, and that further increase of the contact time does not influence the adsorption process. It can be seen that the adsorption process has two distinctive stages, initial process completing in approximately 240 min followed by a slow and marginal uptake extending to several hours. The results of the adsorption experiments indicate that nanocomposites are effective in decreasing the uranium concentration in the effluent. A maximum of 94 % decrease from the initial concentration of 50 mg/L is observed during 240 min of contact time. The initial process is attributed to the adsorption of U(VI) ions on the surface and the second process is due to the slow reduction of uranium from solution [15]. To ensure that equilibrium was established in each case, a contact time of 240 min was selected for all batch adsorption experiments.

The adsorption data were treated according to pseudo first order or pseudo second order kinetic equation [16, 17] to investigate the controlling mechanism of the adsorption process.

The pseudo first order kinetic equation is given as:

$$\ln(Q_{eq} - Q_t) = \ln Q_{eq} - k_1 t \tag{2}$$

where Q_{eq} and Q_t (mg/g) are the amount of U(VI) ions adsorbed at equilibrium and at time (t), k_1(L/min) is the rate constant of pseudo-first-order kinetic equation.

The pseudo second order equation, Ho and Mckay model is expressed as follows:

$$\frac{t}{Q_t} = \frac{1}{k_2 Q_{eq}^2} + \frac{t}{Q_{eq}} \tag{3}$$

where k_2 is the rate constant of pseudo second order kinetic adsorption.

The constants corresponding to the pseudo first/ pseudo second order equations were calculated from the intercept and slope values of the plot (Fig. 9). As seen from Fig. 9B, the pseudo second order equation fits well with the experimental data, and the correlation coefficient obtained for pseudo second order equation is 0.9972. Furthermore, the adsorption capacities calculated by the pseudo second order model are very close to the experimental value. These results suggest that a pseudo second order adsorption is the predominant mechanism.

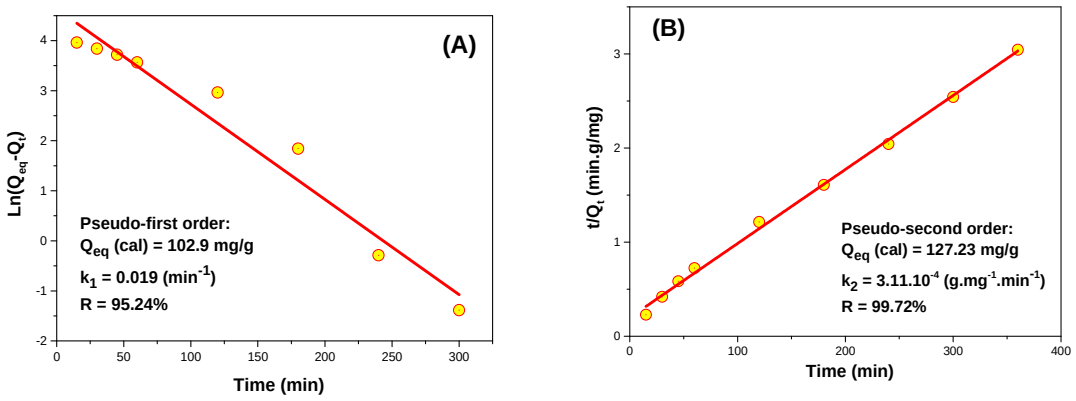

Figure 9. Pseudo-first-order (A), pseudo-second-order (B) plot for the adsorption of uranium.

3.4. Adsorption isotherms

Equilibrium isotherm studies were carried out to evaluate the maximum adsorption capacity of CNF – rGO materials for U(VI). The adsorption capacity of CNF - rGO nanocomposites versus the equilibrium concentration of U(VI) in the aqueous solution is plotted in Fig. 10. The results revealed that the precipitation of uranium species is insignificant even at the highest uranium concentration employed in our studies. The removal of uranium in presence of materials can be assigned to the interaction between materials surface and uranium species present in solution. Under our experimental condition, uranium loading onto the nanocomposites was found to be saturated at approximately 159.5 mg/g.

The data were simulated by the widely used the Langmuir, Freundlich isotherm and Dubinin–Radushkevich models [18, 19, 20] to understand the adsorption mechanism.

The Langmuir equation is:

$$\frac{C_{eq}}{Q_{eq}} = \frac{1}{Q_m} C_{eq} + \frac{1}{K_L Q_m} \tag{4}$$

where Q_m (mg/g) is the Langmuir monolayer adsorption capacity; C_{eq} (mg/L) is the equilibrium concentration; Q_{eq} (mg/g) is the adsorbed amount at equilibrium time; K_L is the Langmuir equilibrium constant.

The formula of Freundlich isotherm is :

$$\ln\ Q_{eq} = \ln K_F + \frac{1}{n} \ln C_{eq} \tag{5}$$

K_F and n are the Freundlich constants related to the adsorption capacity and adsorption intensity, respectively.

The Dubinin–Radushkevich equation is:

$$\ln\ Q_{eq} = \ln Q_m - K_{D\text{-}R}\ \varepsilon^2 \tag{6}$$

where Q_{eq} is the amount of U(VI) adsorbed at the equilibrium, $K_{D\text{-}R}$ is a constant related to the adsorption energy, Q_m is the theoretical saturation capacity, and ε is the Polanyi potential which is equal to:

$$\varepsilon = RT.\ln\left(1+\frac{1}{C_{eq}}\right) \tag{7}$$

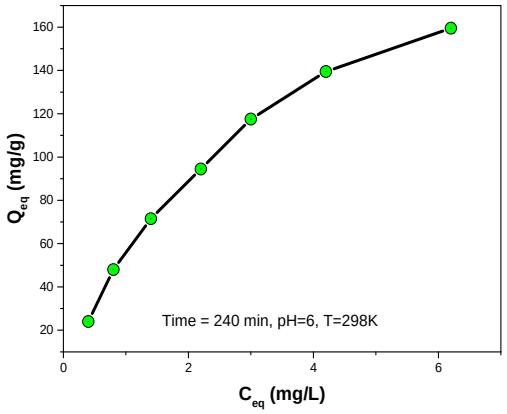

Figure 10. Effect of equilibrium uranium on the adsorption of uranium.

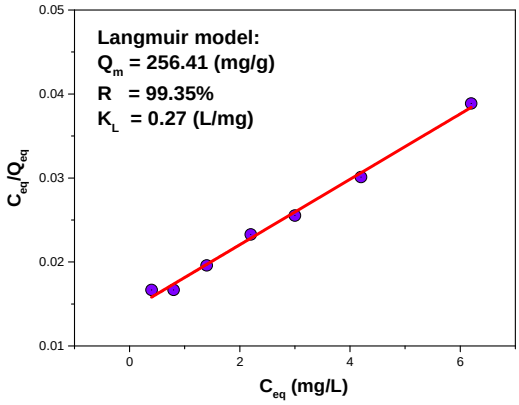

Figure 11. The model fits of Langmuir isotherms for the adsorption of uranium.

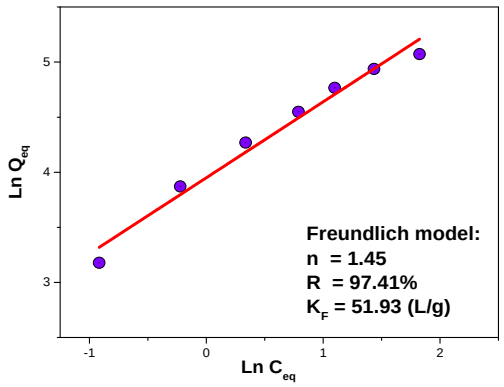

Figure 12. The model fits of Freundlich isotherms for the adsorption of uranium.

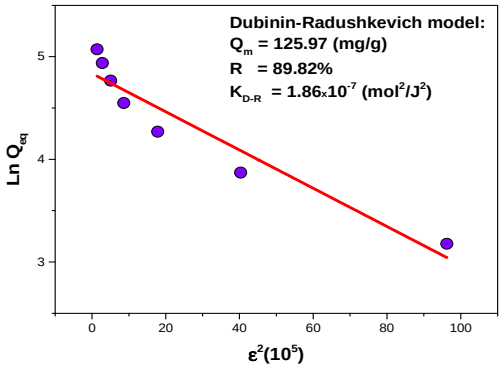

Figure 13. The model fits of Dubinin – Radushkevich isotherms for the adsorption of uranium.

The linear plots of Langmuir, Freundlich and Dubinin – Radushkevich equations representing uranium (VI) adsorption were illustrated in Fig. 11 - 13. Based on high correlation coefficient values, the Langmuir isotherm is most suitable to characterize the uranium adsorption behavior of CNF - rGO materials. The Langmuir model indicates that U(VI) is adsorbed by specific sites of CNF - rGO and forms a monolayer. This also indicates the homogeneity of active sites on the surface of CNF - rGO. The maximum adsorption capacity of CNF - rGO is about 256 mg/g for uranium(VI) at 298K. This value is found to be in general better than those reported in the literature for uranium adsorption [9, 11].

4. CONCLUSION

CNF - rGO nanocomposites have been successfully prepared by the two-steps methods. The CNF - rGO materials could be recovered readily from aqueous solution by magnetic separation. The equilibrium data were well fitted by the Langmuir adsorption isotherm model, and CNF - rGO exhibited high absorbability for U(VI). The maximum adsorption capacity of U(VI) with CNF - rGO nanocomposites was 256 mg/g at pH = 6 and T = 298 K. Findings of the present work to highlight the potential for magnetic graphene nanocomposites as an effective and recyclable adsorbent for the radioactive wastewater treatment.

REFERENCES

1. Zhang X.F., Jiao C.S. and Wang J. - Removal of uranium(VI) from aqueous solution by magnetic Schiff base: Kinetic and thermodynamic investigation, Chemical Engineering Journal **198 - 199** (2012) 412 - 419.
2. Parth D.B., Deepesh P. and Balasubramanian K. - A review of potential remediation techniques for uranium(VI) ion retrieval from contaminated aqueous environment, Journal of Environmental Chemical Engineering **2** (3) (2014) 1621-1634.
3. Situate G.S., Lyuke S.G., Ndlovu S. and Heydenrych M. - The heterogeneous coagulation and flocculation of brewery wastewater using carbon nanotubes, Water Research **46** (2012) 1185 - 1197.
4. Zhao G., Li J., Ren X., Chen C. and Wang X. - Few-layered graphene oxide nanosheets as superior sorbents for heavy metal ion pollution management, Environ. Sci. Technol. **45** (24) (2011) 10454 -10462.
5. Jung G., Lin Z., Chen C., Zhu L., Chang Q., Wang N., Wei W. and Tang H. - TiO_2 nanoparticles assembled on graphene oxide nanosheets with high photocatalytic activity for removal of pollutants, Carbon **49** (2011) 2693 - 2701.
6. Fang L.F., Zhi Q., Jing B., Wei D.R., Fu Y.F., Wei T., Xiao L.W., Yang W. and Liang Z. - Rapid removal of uranium from aqueous solutions using magnetic Fe_3O_4@SiO_2 composite particles, Journal of Environmental Radioactivity **106** (2012) 40 - 46.
7. Makoto T., Shunichi I., Hirotaka T. and Zhenghe X. - Preparation of poly(1-vinylimidazole)-grafted magnetic nanoparticles and their application for removal of metal ions, Chem. Mater. **16** (2004)1977 - 1983.
8. Chun J., Seo S.W., Jung G.Y. and Lee J.W. - Easy access to efficient magnetically recyclable separation of histidine-tagged proteins using superparamagnetic nickel ferrite nanoparticle clusters, Mater. Chem. **21** (18) (2011) 6713 - 6717.
9. Dat T.Q., Vi L.D. and Hung D.Q. - Uranium removal activity of $Cu_{0.5}Ni_{0.5}Fe_2O_4$ superparamagnetic nano particles prepared by large scale method, Journal of Science and Technology **52** (3A) (2014) 66 - 73 (in Vietnamese).
10. Reddy D.H.K. and Yun Y.S. - Spinel ferrite magnetic adsorbents: alternative future materials for water purification?, Coordination Chemistry Reviews **315** (2016) 90 - 111.
11. Cheng W.C., Jin Z.X., Ding C.C. and Wang M.L. - Simultaneous sorption and reduction of U(VI) on magnetite–reduced graphene oxide composites investigated by macroscopic, spectroscopic and modeling techniques, RSC Advances **5** (2015) 59677 - 59685.

12. Bakr A.A., Moustafa Y.M., E.A. Motawea E.A., Yehia M.M. and Khalil M.M.H. - Removal of ferrous ions from their aqueous solutions onto ZNF–rGO – alginate composite beads, J. Env. Chem. Eng. **3** (2015) 1486 - 1496.
13. Hummers W.S., Offeman R.E. - Preparation of Graphitic Oxide, J. Am. Chem. Soc. **80** (6) (1958) 1339 – 1339.
14. Shen J., Hu Y., Shi M., Li N., Ma H., Ye M. - One step synthesis of graphene oxide-magnetic nanoparticle composite, Journal of Physical Chemistry C **114** (2010) 1498 – 1503.
15. Missana C., Maffiotte C. and Gutierrez M.G. - Surface reaction kinetics between nanocrystalline magnetite and uranyl, J. Colloids Interface Sci. **261** (1) (2003) 154 - 160.
16. López F.A., Martín M.I., Pérez C., López-Delgado A. and Alguacil F.J. - Removal of copper ions from aqueous solutions by a steel-making by-product, Water. Res. **37** (2003) 3883 - 3890.
17. Ho Y.S. and McKay G. - Pseudo-second order model for sorption processes, Process Biochem. **34** (1999) 451 - 465.
18. Langmuir I. - The adsorption of gases on plane surfaces of glass, mica and platinum, J. Am. Chem. Soc. **40** (1918) 1361 - 1403.
19. Freundlich H.M.F. - Über die Adsorption in Lösungen, Z. Phys. Chem. **57** (1906) 385 - 470.
20. Akar T., Kaynak Z., Ulusoy S., Yuvaci D., Ozsari G. and Akar S.T. - Enhanced biosorption of nickel (II) ions by silica-gel-immobilized waste biomass characteristics in batch and dynamic flow mode, J. Hazard. Mater. **163** (2009) 1134 - 1141.

TÓM TẮT

HẤP PHỤ URANI TRONG DUNG DỊCH BẰNG NANOCOMPOSIT $Cu_{0.5}Ni_{0.5}Fe_2O_4$ – REDUCED GRAGHENE OXIDE

Trần Quang Đạt*, Nguyễn Văn Toàn, Phạm Văn Thìn, Đỗ Quốc Hùng

Đại học Kỹ thuật Lê Quý Đôn, 236 Hoàng Quốc Việt, Hà Nội

*Email: *dattqmta@gmail.com*

Composit giữa $Cu_{0.5}Ni_{0.5}Fe_2O_4$ – khử graphene oxit (CNF-rGO) - một vật liệu hấp phụ hiệu năng uranium (VI) đã được chế tạo thành công qua hai bước công nghệ. Cấu trúc và tính chất hóa lý của vật liệu được xác định bằng hiển vi điện từ quét (SEM), giản đồ nhiễu xạ tia X (XRD), phổ RAMAN và phép đo từ kế mẫu rung (VSM). Kết quả cho thấy, rGO được bóc tách và được kết hợp với các hạt nano CNF có kích thước cỡ 20 nm. Từ độ bão hòa của mẫu đạt 60 emu/g, còn từ dư và lực kháng từ xấp xỉ không cho thấy vật liệu là siêu thuận từ. Các ảnh hưởng của pH, thời gian hấp phụ, hấp phụ đẳng nhiệt đã được khảo sát. Đường hấp phụ đẳng nhiệt phù hợp với mô hình Langmuir, với dung lượng hấp phụ cỡ 256 mg/g ở *pH* 6, nhiệt độ 298 K.

Từ khóa: rGO, $Cu_{0.5}Ni_{0.5}Fe_2O_4$, nanocomposites, uranium, hấp phụ.